

## Original Research



# Allomyrina dichotoma larva extract attenuates free fatty acid-induced lipotoxicity in pancreatic beta cells

Kyong Kim <sup>1\*</sup>, Min-Kyu Kwak <sup>1\*</sup>, Gong-Deuk Bae <sup>2</sup>, Eun-Young Park <sup>3</sup>,  
Dong-Jae Baek <sup>3</sup>, Chul-Young Kim <sup>4</sup>, Se-Eun Jang <sup>1</sup>, Hee-Sook Jun <sup>5</sup> and  
Yoon Sin Oh <sup>1§</sup>

<sup>1</sup>Department of Food Nutrition, College of Bio Convergence, Eulji University, Seongnam 13135, Korea

<sup>2</sup>Institute of Lee Gil Ya Cancer and Diabetes, Department of Molecular Medicine, Gachon University, Incheon 21999, Korea

<sup>3</sup>College of Pharmacy and Natural Medicine Research Institute, Mokpo National University, Muan 58554, Korea

<sup>4</sup>College of Pharmacy, Hanyang University, Ansan 15588, Korea

<sup>5</sup>College of Pharmacy and Gachon Institute of Pharmaceutical Science, Gachon University, Incheon 21936, Korea

## OPEN ACCESS

**Received:** Jul 27, 2020

**Revised:** Sep 28, 2020

**Accepted:** Dec 9, 2020

### §Corresponding Author:

Yoon Sin Oh

Department of Food and Nutrition, Eulji University, 553 Sanseong-daero, Sujeong-gu, Seongnam 13135, Korea.

Tel. +82-31-740-7287

Fax. +82-31-740-7370

E-mail. ysoh@eulji.ac.kr


\*These authors contributed equally to this study.

©2021 The Korean Nutrition Society and the Korean Society of Community Nutrition  
This is an Open Access article distributed under the terms of the Creative Commons Attribution Non-Commercial License (<https://creativecommons.org/licenses/by-nc/4.0/>) which permits unrestricted non-commercial use, distribution, and reproduction in any medium, provided the original work is properly cited.


### ORCID iDs

Kyong Kim 


<https://orcid.org/0000-0002-8354-0488>

Min-Kyu Kwak 


<https://orcid.org/0000-0003-0295-613X>

Gong-Deuk Bae 


<https://orcid.org/0000-0002-1142-2634>

Eun-Young Park 

<https://orcid.org/0000-0002-4263-201X>

Dong-Jae Baek 

<https://orcid.org/0000-0001-6100-488X>

Chul-Young Kim 

<https://orcid.org/0000-0001-6257-0293>

## ABSTRACT


**BACKGROUND/OBJECTIVES:** *Allomyrina dichotoma* larva (ADL), one of the many edible insects recognized as future food resources, has a range of pharmacological activities. In a previous study, an ADL extract (ADLE) reduced the hepatic insulin resistance of high-fat diet (HFD)-induced diabetic mice. On the other hand, the associated molecular mechanisms underlying pancreatic beta-cell dysfunction remain unclear. This study examined the effects of ADLE on palmitate-induced lipotoxicity in a beta cell line of a rat origin, INS-1 cells.

**MATERIALS/METHODS:** ADLE was administered to high-fat diet treated mice. The expression of apoptosis-related molecules was measured by Western blotting, and reactive oxidative stress generation and nitric oxide production were measured by DCH-DA fluorescence and a Griess assay, respectively.

**RESULTS:** The administration of ADLE to HFD-induced diabetic mice reduced the hyperplasia, 4-hydroxynonenal levels, and the number of apoptotic cells while improving the insulin levels compared to the HFD group. Treatment of INS-1 cells with palmitate reduced insulin secretion, which was attenuated by the ADLE treatment. Furthermore, the ADLE treatment prevented palmitate-induced cell death in INS-1 cells and isolated islets by reducing the apoptotic signaling molecules, including cleaved caspase-3 and PARP, and the Bax/Bcl2 ratio. ADLE also reduced the levels of reactive oxygen species generation, lipid accumulation, and nitrite production in palmitate-treated INS-1 cells while increasing the ATP levels. This effect corresponded to the decreased expression of inducible nitric oxide synthase (*iNOS*) mRNA and protein.

**CONCLUSIONS:** ADLE helps prevent lipotoxic beta-cell death in INS-1 cells and HFD-diabetic mice, suggesting that ADLE can be used to prevent or treat beta-cell damage in glucose intolerance during the development of diabetes.

**Keywords:** Diabetes mellitus; apoptosis; insulin-secreting cells; nitric oxide; oxidative stress

Se-Eun Jang 
<https://orcid.org/0000-0003-3279-0871>

 Hee-Sook Jun 
<https://orcid.org/0000-0002-1166-4932>

 Yoon Sin Oh 
<https://orcid.org/0000-0003-3995-4429>

#### Funding

This study was supported by the Basic Science Research Program grant (NRF-2018R1C1B6000998) provided by the National Research Foundation of Korea (NRF) funded by the Ministry of Science, ICT.

#### Conflict of Interest

The authors declare no potential conflicts of interests.

#### Author Contributions

Conceptualization: Kim K, Kwak MK, Bae GD, Kim CY, Jun HS, Oh YS; Data curation: Kim K, Kwak MK, Bae GD, Kim CY, Jun HS, Oh YS; Formal analysis: Kim K, Kwak MK, Bae GD, Kim CY, Jun HS; Investigation: Park EY, Baek DJ, Jang SE; Project administration: Oh YS; Supervision: Oh YS; Writing - original draft: Kim K, Kwak MK, Bae GD, Kim CY, Jun HS, Oh YS; Writing - review & editing: Oh YS.

## INTRODUCTION

Chronic insulin resistance and a progressive decline in the beta-cell mass and function are two of the key causes of type 2 diabetes. Therefore, an optimal beta-cell mass and function are essential for glucose homeostasis. On the other hand, impaired glucose homeostasis leads to the progression of diabetes. Increased free fatty acids (FFA), in particular saturated FFA (e.g., palmitate and stearate), have been suggested to trigger type 2 diabetes through the induction of beta-cell apoptosis and dysfunction [1]. The apoptotic process is initiated by the intrinsic or mitochondrial pathways. Therefore, the loss of mitochondrial homeostasis induces the release of pro-apoptotic factors, including cytochrome c, which activates the caspase proteins (caspase-3 and caspase-9) [2]. Permeabilization of the mitochondrial membrane and the release of cytochrome c are regulated tightly by a group of proteins called the Bcl2 protein family (anti-apoptotic members, Bcl2 and Bcl-XL; pro-apoptotic members, Bax, Bak, Bad, and Bim) [3]. The precise mechanisms of these proteins are well characterized. Their specific interactions and the ratio between anti- and pro-apoptotic proteins play important roles in determining the fate of cells exposed to apoptotic stimuli [4].

Several studies have reported the mechanisms of fatty acid-induced lipotoxicity in pancreatic beta cells during the development of type 2 diabetes. On the other hand, many proposed models, such as those including FFA receptors and the cell stress response, comprised of ceramide formation, lipid droplet formation, endoplasmic reticulum stress, mitochondrial dysfunction, and autophagy, continue to be investigated [5]. Therefore, the inhibition or prevention of these mechanisms is likely to play an important role in developing new anti-diabetic drugs that target beta cells.

Insects have been proposed as an alternative food source to curb the increasing global demand for protein consumption. Recently, pharmacological studies on the value of insects as an alternative food source have been reported. In Korea, silkworms (*Bombyx mori*) and locusts are readily accepted as general food items [6,7]. Prompted by new Korean legislation regarding insect industries in 2010, an edible insect industry now exists on a commercial scale, but it is currently in its initial stages. The Korean horn beetle (*Allomyrina dichotoma*), one of five insects permitted for food and feed in Korea, is used in traditional medicine for its anti-hepatofibrotic, anti-neoplastic, anti-obesity, and anti-diabetic effects [8]. The pharmacological properties have been primarily reported in beetle larva [9]. A recent study reported that the ethanol extract from *Allomyrina dichotoma* larva (ADL) mitigated hepatic insulin resistance in high-fat diet-induced diabetic mice and inhibited hepatic lipogenesis via activation of the AMPK signaling pathway, a mechanism associated with the effects elicited by *A. dichotoma* larva extract (ADLE). To determine if ADLE can act directly against lipotoxicity, this study examined the effects of beta-cell apoptosis and glucose-stimulated insulin secretion in palmitate-induced lipotoxicity, as well as its associated molecular mechanisms.

## MATERIALS AND METHODS

### Preparation of ADLE

After a week of fasting to remove feces, dried ADL were purchased from Yechun Bug's Land (Yecheon, Korea). ADL (200 g) was extracted, as previously reported [10], and the resulting concentrates were lyophilized to obtain ADLE. The calculated yield mean was 11.84%

compared to the powdered sample. Finally, ADLE was dissolved in deionized water for subsequent experiments.

### Cell culture and treatment

The rat insulinoma cell line, INS-1, was cultured in RPMI 1640 medium (Gibco, Paisley, UK) supplemented with 1% penicillin/streptomycin (Welgene, Daegu, Korea) and 10% fetal bovine serum (Gibco) in a 5% CO<sub>2</sub> environment at 37°C. To induce lipotoxicity, sodium palmitate (Sigma, St. Louis, MO, USA) was conjugated with 5% bovine serum albumin (BSA; Sigma) at a 1:3 volume ratio. The INS-1 cells were exposed to palmitate (0.4 mM), with or without ADLE (0.5 mg/mL), for 24 h. The cell cytotoxicity on ADLE was determined by colorimetry using MTT (thiazolyl blue) (Duchefa Biochemie BV, Haarlem, Netherlands). The insoluble purple formazan products were dissolved in 2-propanol and measured at 540 nm (TECAN Group Ltd., Shanghai, China).

### Animal experiments

Four-week-old C57BL/6J male mice were purchased from the Korea Research Institute Bioscience & Biotechnology (KRIBB, Daejeon, Korea). Male mice were chosen because they have been reported to be affected more by glucose intolerance than their female counterparts. Hence, they are employed more often in diet-induced obesity studies [11-13]. After one week of adaptation, the high-fat diet (HFD, 60% fat, D12492; Research Diets, New Brunswick, NJ, USA) and the normal fat diet (NFD, 4.5% fat, Purina, n = 6) were provided to the mice for 6 weeks. The HFD-fed mice were divided into 2 groups by a stratified randomized design based on the blood glucose level (200–250 mg/dL). The mice were then treated orally with ADLE (100 mg/kg/day, n = 8) [10,14,15] or vehicle (distilled water, n = 8) once a day for 6 weeks using a flexible plastic feeding tube, as described elsewhere [10]. After the experimental period, all mice were euthanized after a 12-h fasting period, and the pancreatic tissue was either snap-frozen or processed for histopathology. All animal procedures were approved by the Eulji University Institutional Animal Care and Use Committee (EUIACUC-18-7).

### Islet isolation

Male Sprague-Dawley rats (weighing 200 g) were purchased from KRIBB. The islets were isolated by infusing collagenase P into the pancreas (Roche Diagnostics, Indianapolis, IN, USA), followed by separation using a Histopaque 1077 gradient (Sigma) [16]. After isolation, the morphologically intact islets were selected under a stereomicroscope. The isolated islets were then treated with trypsin-ethylenediaminetetraacetic acid to obtain single cells before being seeded on a 96-well plate at a density of  $5.0 \times 10^4$  cells/well. After overnight stabilization, the cells were treated with palmitate, with or without ADLE, for 24 h.

### Histology of pancreas tissues

Paraffin-embedded pancreas sections (4 μm) were fixed in acetone and deparaffinized, followed by staining with hematoxylin and eosin (H&E). For the immunohistochemical detection of insulin and 4-hydroxynonenal (4-HNE), the pancreas sections were incubated with the following primary antibodies: rabbit anti-insulin (1:1,000; ab63820; Abcam, Cambridge, UK), and rabbit anti-4-HNE (1:1,000, ab46545; Abcam), followed by treatment with HRP-conjugated secondary antibody (Bio-Rad, Marnes-la-Coquette, France). Apoptosis was measured by staining sections with terminal deoxynucleotidyl transferase dUTP nick end labeling (TUNEL) according to the manufacturer's instructions using an *in situ* cell death detection kit (Roche Diagnostics GmbH, Mannheim, Germany). The TUNEL-positive cells

in randomly selected islets of each mouse were counted under a microscope. The pancreas sections were observed using an Olympus BX61 microscope equipped with an Olympus DP70 digital camera (Olympus Co., Tokyo, Japan). The beta-cell area (pixels) on insulin-stained sections was quantified using the Image J software (National Institutes of Health, Bethesda, MD, USA). The insulin-positive area of all islets was measured, and the area was calculated by dividing the number of islets.

### Assay for apoptotic cell death

The levels of the cytoplasmic histone-associated DNA fragments were determined using the Cell Death Detection enzyme-linked immunosorbent assay (ELISA) Plus kit (Roche Molecular Biochemicals, Mannheim, Germany). The cells were washed with Dulbecco's phosphate-buffered saline (DPBS) and lysed by adding the buffer supplied with the kit. Following centrifugation ( $200 \times g$ , 10 min), the supernatant containing the cytoplasmic fraction was used in ELISA and processed according to the manufacturer's protocol. After incubating with a peroxidase substrate for 5 min, the absorbances at 405 and 490 nm (reference wavelength) were measured using a microplate ELISA reader (Tecan).

### Cellular lipids measurement

The lipid contents in the cell were measured using the method reported by Folch *et al.* [17]. Briefly, INS-1 cells in 6-well plates were digested with trypsin, and the lysates were centrifuged at  $72 \times g$  for 3 min. A chloroform/methanol mixture (2:1 v/v) was then added. A 0.1 M NaCl was added to each group. The mixture was centrifuged at  $1,530 \times g$  for 10 min, and the bottom layer was dried. The 1% Triton X-100-ethanol was added, and the concentration of lipid was measured using a TG-S (triglyceride) kit (Asan Pharmaceutical Co., Seoul, Korea) according to the manufacturer's instructions. The data were normalized for differences by the protein content of the cell.

### Measurement of insulin secretion

The plasma insulin levels in each group were measured after fasting the mice overnight before collecting blood samples from the tail vein (0 min). Subsequently, a glucose solution (2 g/kg) dissolved in phosphate-buffered saline (PBS) was injected intraperitoneally. Another blood sample was collected at 30 min. The levels of insulin secretion in the ADLE-treated cells were measured. INS-1 cells were plated ( $2.0 \times 10^5$  cells/well) in 24-well plates. Glucose-stimulated insulin secretion (GSIS) within the cells was then performed as follows. The cells were equilibrated overnight in RPMI 1640 medium containing 5.0 mM glucose. The cells were washed with Krebs–Ringer bicarbonate (KRB) buffer (119 mM NaCl, 4.74 mM KCl, 2.54 mM  $\text{CaCl}_2$ , 1.19 mM  $\text{KH}_2\text{PO}_4$ , 25 mM  $\text{MgHCO}_3$ , and 10 mM HEPES at pH 7.4, containing 0.2% BSA) and pre-incubated for 2 h in the same buffer. Insulin secretion was stimulated by treating the cells with KRB buffer containing 3.3 mM or 25 mM glucose for 2 h at  $37^\circ\text{C}$ . The supernatants were collected, and the amount of insulin released was measured using an ELISA kit according to the manufacturer's protocol (Alpco Diagnostics, Windham, NH, USA). The insulin content was normalized to the protein levels extracted from the cells.

### Measurement of the nitrite content

The nitrite concentration in the extracellular space was measured using a colorimetric assay to determine the levels of nitric oxide (NO) production. The cells at a density of  $2.5 \times 10^4$  cell/well were cultured in palmitate with or without ADLE for 24 h. The levels of NO production in the medium were measured after incubating the cells with an equal volume of Griess reagent (1%

sulfanilamide/0.1% N-(1-naphthyl)-ethylenediamine dihydrochloride/2.5% H<sub>3</sub>PO<sub>4</sub>) at 23–25°C for 10 min. The absorbance at 540 nm was measured using a microplate reader (TECAN).

### Measurement of intracellular reactive oxygen stress

The levels of intracellular reactive oxygen species (ROS) were assessed using an oxidative-sensitive 2', 7'-dichloro dihydrofluorescein diacetate (DCFH-DA; Molecular Probes, Thermo Fisher Scientific, Waltham, MA, USA) fluorescent probe. The cells at a density of  $2.5 \times 10^4$  cells/well were cultured in palmitate with or without ADLE for 24 h. The cells were incubated with 10  $\mu$ M DCFH-DA in the dark for 30 min. The fluorescence of dichlorofluorescein (DCF) in the cells was detected using a fluorescence spectrophotometer with excitation and emission at 488 nm and 535 nm, respectively.

### Measurement of cellular ATP

INS-1 cells at a density of  $2.5 \times 10^4$  cell/well were cultured in palmitate in 96 opaque black-well plates for 24 h. The adenosine triphosphate (ATP) levels in the cells were measured using a Perkin-Elmer ATPLite system according to the manufacturer's instructions.

### Western blot analysis

The cell lysates were homogenized in mammalian protein extraction buffer (Sigma). The resulting lysates were centrifuged at 12,000 rpm, and 4°C for 15 min, and the protein contents were measured using a protein-assay dye reagent concentrate (Bio-Rad Laboratories, Hercules, CA, USA). Subsequently, 10–15% sodium dodecyl sulphate-polyacrylamide gel electrophoresis was performed, followed by transfer onto nitrocellulose blotting membranes (Amersham, GE Healthcare Life Science, Germany). The antibodies used for immunoblotting are as follows: Bax rabbit mAb (1:1,000; Cell Signaling Technology), Bcl2 (D17C4) rabbit mAb (1:1,000; Cell Signaling Technology), inducible nitric oxide synthase (iNOS; NOS2) (1:500; Santa Cruz Biotechnology, Santa Cruz, CA, USA), AMPK $\alpha$  (D63G4) rabbit mAb (1:1,000; Cell Signaling Technology), Phospho-AMPK $\alpha$  (Thr172) (D4D6D) rabbit mAb (1:1,000; Cell Signaling Technology), caspase-3 rabbit mAb (1:1,000; Cell Signaling Technology), cleaved caspase-3 (Asp175) (5A1E) rabbit mAb (1:1,000; Cell Signaling Technology), PARP (46D11) rabbit mAb (1:1,000; Cell Signaling Technology), and  $\beta$ -actin (13E5) rabbit mAb (1:2,500; Cell Signaling Technology). The protein bands were visualized using an enhanced chemiluminescence method with an ELC kit (Millipore, Billerica, MA, USA) and were quantified using Quantity 1 v.4.6.7 (Bio-Rad).

### Quantitative real-time polymerase chain reaction (qRT-PCR)

The total RNA was extracted from the cultured cells using Trizol reagent (Invitrogen, Grand Island, NY, USA), and cDNA was synthesized using a Primescript™ 1st strand cDNA synthesis kit (Takara Bio Inc., Shiga, Japan). mRNA expression was measured by qRT-PCR using SYBR Premix Ex Taq II ROX plus (Takara Bio Inc.) and an ABI real-time PCR system (Applied Biosystem Inc., Foster City, CA, USA). **Table 1** lists the gene-specific primers. Cyclophilin was used as the internal control. PCR was carried out for 40 cycles (10 min at 90°C, 15 s at 95°C, and 1 min at 60°C). The relative amounts of mRNAs were calculated using the threshold crossing points (CT) based on the  $2^{-\Delta\Delta C_t}$  method.

### Statistical analysis

All data are presented as the mean  $\pm$  SD. Statistical analyses were performed using SPSS 20.0 software (IBM SPSS ver. 20.0.0 for Windows; IBM Co., Armonk, NY, USA). The significance of the differences among the groups was analyzed using one-way or two-way analysis of

**Table 1.** Primer sequences for real-time PCR

| Gene symbol | Primer sequence                  |
|-------------|----------------------------------|
| BAX         | F: 5'-AGACACCTGAGCTGACCTTGA-3'   |
|             | R: 5'-CGGAGACACTCGCTCAGCTT-3'    |
| BCL2        | F: 5'-GGGATGCCTTTGTGGAACATATG-3' |
|             | R: 5'-CAGCCAGGAGAAATCAAACAGA-3'  |
| iNOS        | F: 5'-CTCACTGTGGCTGTGGTCACCTA-3' |
|             | R: 5'-GGGTCTTCGGGCTTCAGGTTA-3'   |
| CYCLOPHILIN | F: 5'-GGTCTTTGGGAAGGTGAAAGAA-3'  |
|             | R: 5'-GCCATTCTGGACCCAAAA-3'      |

PCR, polymerase chain reaction; BAX, Bcl-2-associated X; BCL2, B cell lymphoma 2; iNOS, inducible nitric oxide synthase.

variance (ANOVA) with Fisher's Least Significant Difference (LSD) comparisons test. *P* values < 0.05 were considered significant.

## RESULTS

### ADLE reduces oxidative stress and apoptosis in the islets from HFD-induced diabetic mice

A previous study confirmed that the fasting blood glucose level and glucose intolerance in HFD-induced diabetic mice was reduced significantly by an ADLE treatment [10]. Therefore, this study investigated whether changes in the beta-cell morphology occurred or if any associated dysfunction was present in these groups using immunohistochemistry (Fig. 1A).

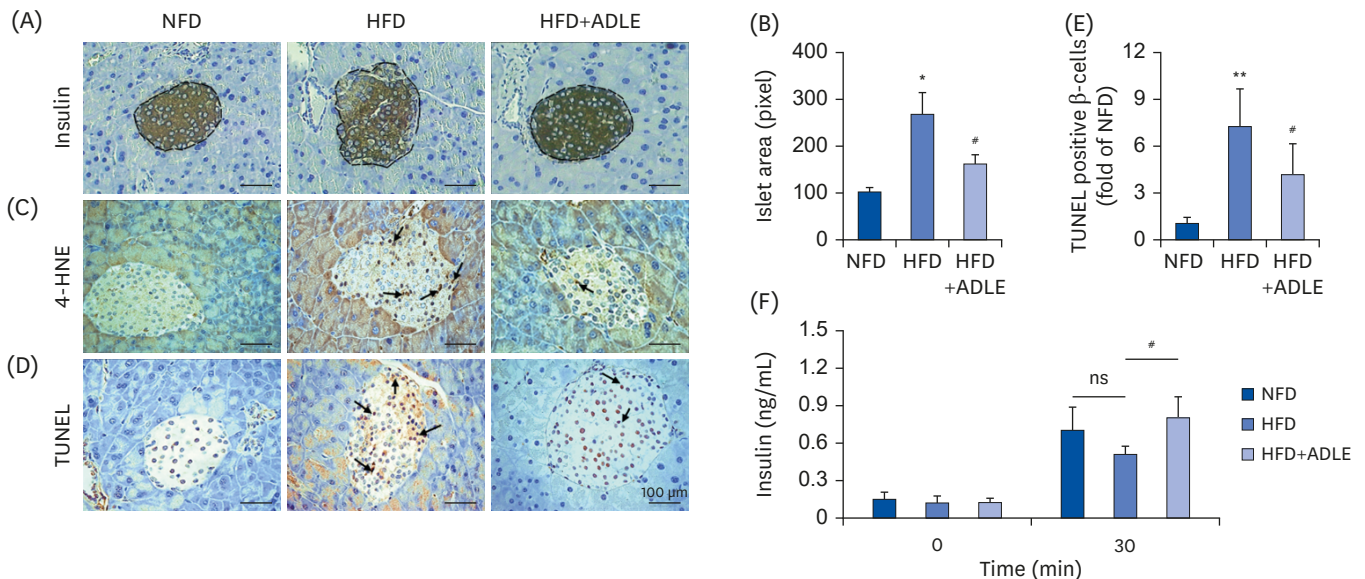


**Fig. 1.** ADLE reduces oxidative stress and apoptosis in the islets from high fat diet-induced diabetic C57BL/6J mice. (A) Representative photomicrographs of immune-staining for insulin (brown color) in pancreatic islets. (B) Measurement of the density of the insulin in the islet area (pixel). (C) Representative photomicrographs of mice pancreatic sections stained with the 4-HNE antibody. (D) Representative photomicrographs of TUNEL-positive cells in pancreatic sections. (E) Histogram representing the quantitative analysis of TUNEL-positive  $\beta$  cells per islet in each experimental group. (F) Plasma serum level at 0 and 30 min after glucose injection (2 g/kg) collected for insulin detection with ELISA (magnification:  $\times 200$ ). Data are presented as the mean  $\pm$  SD ( $n = 5-8$ ). The arrows indicated the 4-HNE and TUNEL stained cells. The significance was evaluated using ANOVA with the LSD comparisons test.

ADLE, *Allomyrina dichotoma* larva extract; NFD, normal fat diet group; HFD, high-fat diet group; HFD+ADLE, high-fat diet plus 100 mg/kg/day ADLE; 4-HNE, 4-hydroxynonenal; TUNEL, terminal deoxynucleotidyl transferase dUTP nick end labeling; ANOVA, analysis of variance; LSD, Least Significant Difference; ns, no significance.

\**P* < 0.05 and \*\**P* < 0.01 versus NFD; #*P* < 0.05 versus HFD.

An examination of the pancreatic islet morphology showed that the size of the islet boundary was expanded significantly with an irregular shape in the HFD group compared to the NFD group, and was improved substantially by ADLE. Quantitative analysis of the insulin-positive cells showed that the beta-cell area increased due to the HFD, whereas the ADLE treatment reduced the beta-cell area (**Fig. 1B**). The changes in the oxidative stress related-factor in the islets from HFD- and ADLE-treated mice were investigated by immunostaining with an antibody against 4-HNE, a marker of oxidative stress [18,19]. The level of 4-HNE (brown color) was observed in the islets of the HFD-fed mice compared to the NFD group. The ADLE-treated group significantly attenuated the HFD-induced oxidative stress (**Fig. 1C**). As shown in **Fig. 1D**, a significant increase in the number of TUNEL-positive cells in the pancreas islets of the HFD-fed mice was observed compared to the NFD-fed mice ( $P < 0.01$ ), and the number was reduced by the ADLE treatment ( $P < 0.01$  vs. HFD group, **Fig. 1D and E**). The plasma insulin levels were also examined upon fasting (0 min) and after 30 min of glucose loading in these groups. Insulin release upon fasting did not differ significantly between the three groups. On the other hand, the HFD+ADLE group showed a significant increase in the circulating insulin levels compared to the HFD group at 30 min after the glucose loading (**Fig. 1F**).

### ADLE attenuates cytotoxicity and lipid accumulation in palmitate-stimulated INS-1 cells

The molecular mechanism associated with the recovery of the beta-cell mass and improved insulin level was determined by assessing the cytotoxicity and intracellular lipid accumulation following treatment with ADLE using rat-derived beta cells. As shown in **Fig. 2A**, the INS-1 cells exhibited cytotoxicity ( $P < 0.001$ ) at a concentration of 1.0 or 2.0 mg/mL ADLE compared to the untreated control. Therefore, this study examined whether ADLE protects INS-1 cells and isolated islets against palmitate-induced cytotoxicity. To this end, the cells were treated with palmitate with or without ADLE (0.1, 0.25, and 0.5 mg/mL). Treatment of INS-1 cells with palmitate decreased the percentage of viable cells to 55.4% compared to the control. In contrast, treatment with ADLE at 0.5 mg/mL in the presence of palmitate increased the cell viability to approximately 71.2% ( $P < 0.001$ ; **Fig. 2B**). Similarly, in isolated islets, ADLE at 0.5 mg/mL significantly increased the cell viability compared to palmitate treatment alone ( $P < 0.05$ ; **Fig. 2C**). The palmitate treatment also resulted in approximately 2.2-fold higher intracellular TG levels than the untreated controls, which was attenuated by the ADLE co-treatment. The ADLE only treatment did not affect the accumulation of triglycerides in the cells (**Fig. 2D**).

### ADLE treatment partially improves insulin secretion via AMPK activation in INS-1 cells

To determine if the ADLE treatment reduced the beta-cell dysfunction induced by palmitate, the levels of insulin secretion were measured in the presence of 3 and 25 mM glucose following a treatment with palmitate with or without ADLE. Insulin secretion increased approximately two-fold with 25 mM glucose compared to 3 mM glucose in the control cells. Insulin secretion after treatment with 3 and 25 mM glucose was significantly lower in the palmitate-treated cells than the untreated control cells. On the other hand, treatment with ADLE ( $P < 0.05$  and  $P < 0.001$ ) enhanced the insulin secretion significantly compared to palmitate (**Fig. 3A**). Previously, the administration of ADLE could increase the AMP-activated kinase (AMPK) activity in the liver of HFD-fed mice [10]. Therefore, the effects of ADLE on AMPK activation were investigated in palmitate-treated INS-1 cells with or without ADLE. The results showed that palmitate reduced the expression of phosphorylated AMPK at Thr 172 (p-AMPK) ( $P = 0.003$ ). In contrast, pretreatment with ADLE improved AMPK phosphorylation in palmitate-treated cells ( $P = 0.04$ ), particularly at 17 h (**Fig. 3B**).

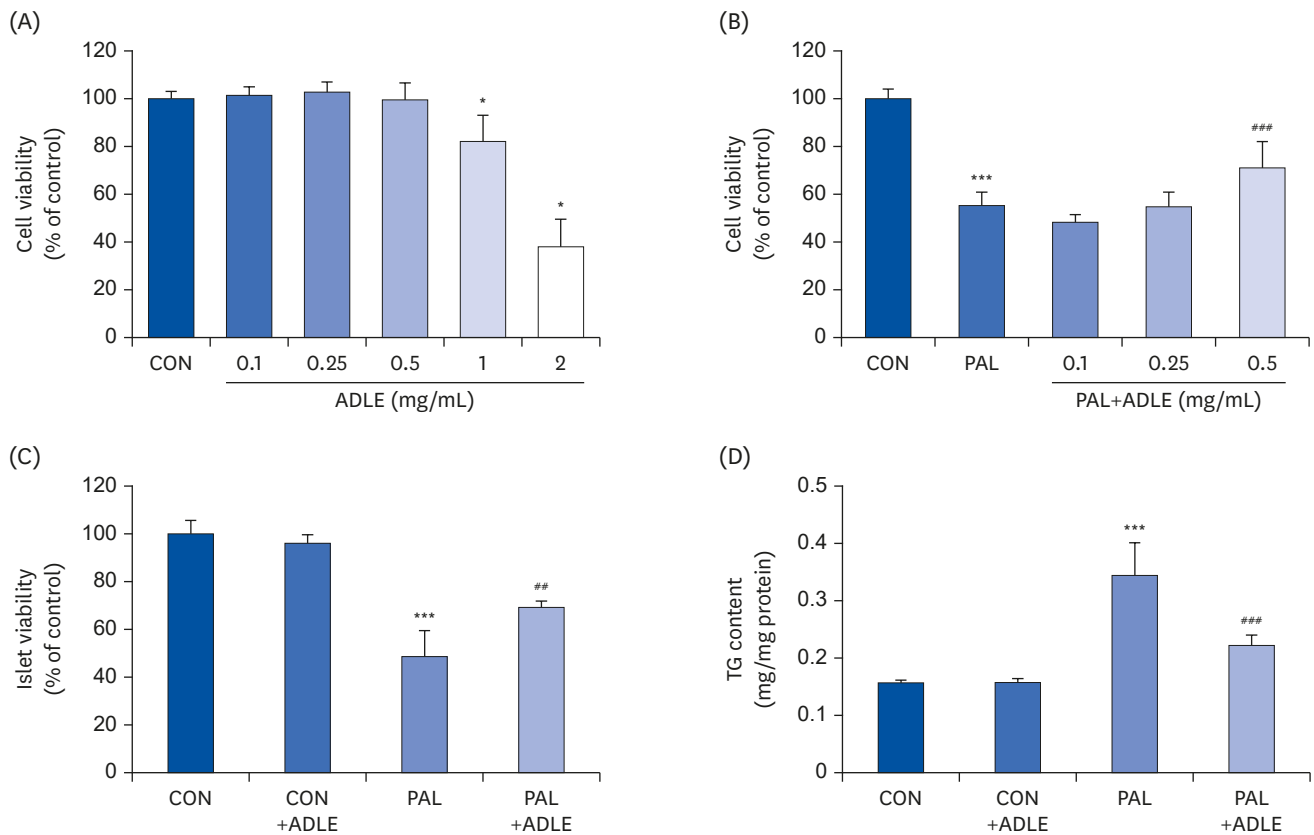


**Fig. 2.** ADLE attenuates cytotoxicity and lipid accumulation in palmitate-stimulated INS-1 cells. (A) Effects of ADLE on the proliferation of INS-1 cells. The cells were incubated in media containing various concentrations of ADLE (0.1, 0.25, 0.5, 1.0, and 2.0 mg/mL) for 24 h. The cell viability was measured using an MTT assay. (B) INS-1 cells were treated with 0.4 mM PAL with or without 0.1, 0.25, and 0.5 mg/mL of ADLE. (C) Rat pancreatic islets were treated with 0.4 mM PAL with or without 0.5 mg/mL of ADLE. The cell viability at 24 h was determined using an MTT assay. (D) The intracellular lipid levels were measured using a triglyceride assay kit. The values are presented as the mean  $\pm$  SD ( $n = 3-5$ ). The significance was evaluated using ANOVA with the LSD comparisons test. ADLE, *Allomyrina dichotoma* larva extract; CON, untreated control; PAL, 0.4 mM palmitate only; CON+ADLE, untreated control plus 0.5 mg/mL ADLE; PAL+ADLE, 0.4 mM palmitate plus 0.5 mg/mL ADLE; MTT, methyl thiazolyl diphenyl tetrazolium; TG, triglyceride; ANOVA, analysis of variance; LSD, Least Significant Difference; ns, no significance. \* $P < 0.05$  and \*\*\* $P < 0.001$  versus CON; \*\* $P < 0.01$  and \*\*\*\* $P < 0.001$  versus PAL.

### ADLE treatment reduces palmitate-induced apoptosis in INS-1 cells

Because palmitate induces apoptosis in pancreatic beta cells [20,21], the effects of ADLE on INS-1 cells were investigated based on the changes in the expression of apoptosis-related proteins. Western blot analysis revealed the cleaved form of caspase-3 and poly-(ADP-ribose)-polymerase (PARP) after the palmitate treatment ( $P = 0.02$ , **Fig. 4A**), but their expression was reduced significantly after the ADLE treatment ( $P = 0.017$ , **Fig. 4B**).

The nucleosomal release was measured for the quantitative analysis of apoptosis. Palmitate-treated cells showed significantly higher nucleosome levels in the cytoplasm due to DNA degradation than the control ( $P < 0.001$ ). The ADLE inhibited the palmitate-mediated nucleosomal release significantly ( $P < 0.01$ ) (**Fig. 4C**). Apoptosis signaling occurs by downregulating Bcl2 expression and upregulating pro-apoptotic Bax expression. As a result, the ratio of the *Bax/Bcl2* mRNA levels was increased two-fold in the palmitate-treated cells than the control ( $P < 0.001$ ). ADLE reduced the mRNA levels significantly ( $P < 0.01$ ) compared to palmitate (**Fig. 5A**). Moreover, the Bax/Bcl2 protein ratio was increased 1.9-fold in the palmitate-treated cells compared to the control ( $P < 0.001$ ). ADLE inhibited the increase in this ratio induced by palmitate significantly ( $P < 0.01$ ) (**Fig. 5B**).



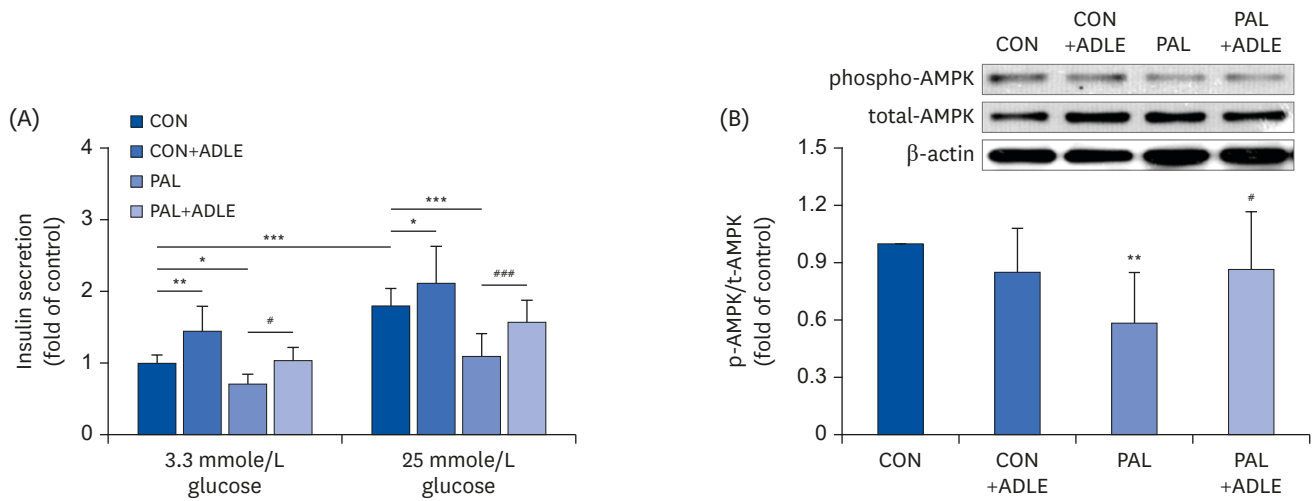


**Fig. 3.** ADLE treatment partially improves insulin secretion via AMPK activation in INS-1 cells. (A) Insulin release was measured after 2 h of incubation in either 3.3 mmol/L glucose or 25 mmol/L glucose, as described in materials and methods. (B) The expression levels of total-AMPK and phospho-AMPK were measured by western blot analysis.  $\beta$ -actin was used as the loading control. The bands were quantified using Quantity 1 software. The data are presented as the mean  $\pm$  SD ( $n = 3-5$ ). The significance was evaluated using an ANOVA with the LSD comparisons test. ADLE, *Allomyrina dichotoma* larva extract; CON, untreated control; PAL, 0.4 mM palmitate only; CON+ADLE, untreated control plus 0.5 mg/mL ADLE; PAL+ADLE, 0.4 mM palmitate plus 0.5 mg/mL ADLE; AMPK, AMP-activated protein kinase; ANOVA, analysis of variance; LSD, Least Significant Difference. \* $P < 0.05$ , \*\* $P < 0.01$ , and \*\*\* $P < 0.001$  versus CON, # $P < 0.05$  and ### $P < 0.001$  versus PAL.

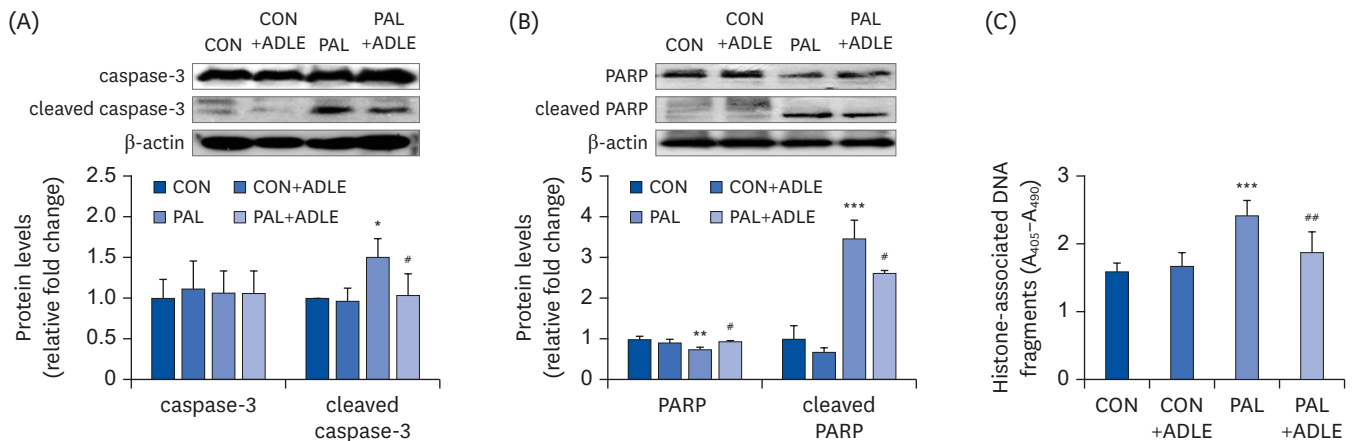


**Fig. 4.** ADLE treatment reduces the expression level of the apoptosis-associated proteins and DNA fragmentation in palmitate-treated INS-1 cells. (A) INS-1 cells were treated with 0.5 mg/mL ADLE and 0.4 mM PAL. The cells were evaluated 24 h after treatment. The whole protein lysates were prepared using an extraction buffer. The levels of caspase-3 (A) and PARP (B) were determined by Western blot analysis with anti-caspase-3 and anti-PARP antibodies, respectively. (C) Fragmented DNA was then measured using a Cell Death Detection ELISA kit. The data are presented as the mean  $\pm$  SD ( $n = 3-5$ ).  $\beta$ -actin was used as the loading control. The bands were quantified using Quantity 1 software. Significance was evaluated using an ANOVA with an LSD comparisons test. ADLE, *Allomyrina dichotoma* larva extract; CON, untreated control; PAL, 0.4 mM palmitate only; CON+ADLE, untreated control plus 0.5 mg/mL ADLE; PAL+ADLE, 0.4 mM palmitate plus 0.5 mg/mL ADLE; PARP, poly (ADP-ribose) polymerase; ELISA, enzyme-linked immunosorbent assay; ANOVA, analysis of variance; LSD, Least Significant Difference. \* $P < 0.05$ , \*\* $P < 0.01$ , and \*\*\* $P < 0.001$  versus CON, # $P < 0.05$  and ### $P < 0.001$  versus PAL.

### ADLE treatment partially prevents ROS generation and restores the ATP levels reduced by palmitate in INS-1 cells

Chronic exposure to palmitate impairs glucose-stimulated insulin secretion with increased ROS production in beta cells [22]. Therefore, to determine if the levels of ROS in palmitate-induced cells were reduced by ADLE treatment, the intracellular ROS levels were measured based on the DCF fluorescence intensity after a treatment with palmitate in the presence or absence of ADLE. Exposure to palmitate alone induced a significant increase in the DCF

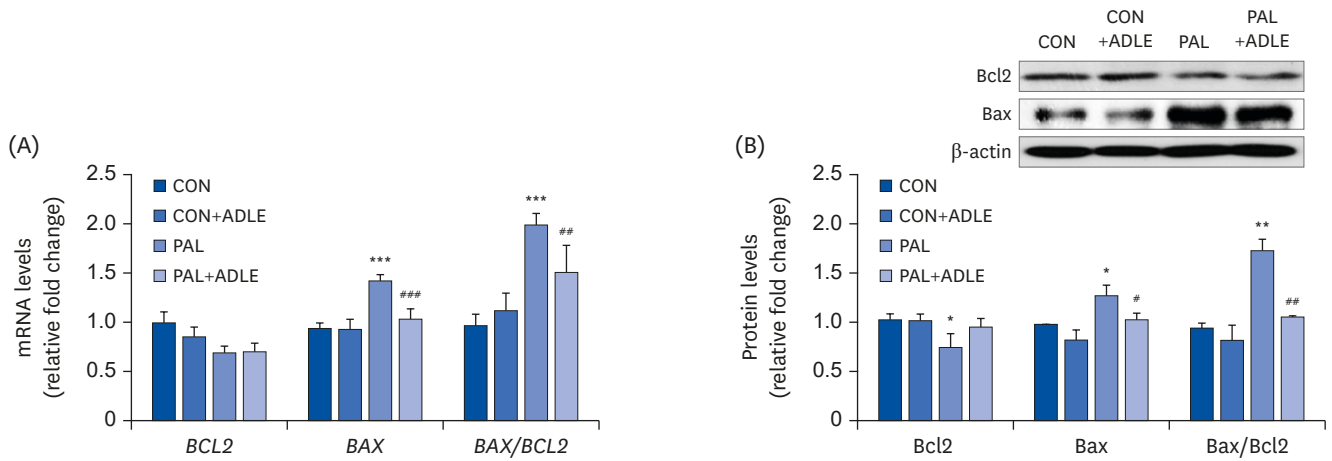


**Fig. 5.** ADLE treatment reduces the Bax/Bcl2 ratio in palmitate-treated INS-1 cells. (A) INS-1 cells were treated with 0.4 mM PAL in the absence or presence of 0.5 mg/mL ADLE. The cells were harvested after 24 h of treatment. The mRNA levels of *BCL2* and *BAX* proteins were analyzed by qRT-PCR. The mRNA levels were normalized with those of cyclophilin. (B) The cells were treated as described in (A) and harvested after a 24 h treatment. The levels of Bcl2 and Bax expression were measured by western blot analysis.  $\beta$ -actin was used as the loading control. The bands were quantified using Quantity 1 software. The values represent the mean  $\pm$  SD ( $n = 3-5$ ). The significance was evaluated using an ANOVA with the LSD comparisons test. ADLE, *Allomyrina dichotoma* larva extract; *BCL2*, B cell lymphoma 2; *BAX*, Bcl-2-associated X; CON, untreated control; PAL, 0.4 mM palmitate only; qRT-PCR, quantitative real-time polymerase chain reaction; CON+ADLE, untreated control plus 0.5 mg/mL ADLE; PAL+ADLE, 0.4 mM palmitate plus 0.5 mg/mL ADLE; ANOVA, analysis of variance; LSD, Least Significant Difference. \* $P < 0.05$ , \*\* $P < 0.01$ , and \*\*\* $P < 0.001$  versus CON. # $P < 0.05$ , ## $P < 0.01$ , and ### $P < 0.001$  versus PAL.

fluorescence levels, which was prevented ( $P < 0.001$ ) by exposure to ADLE (Fig. 6A). A mitochondrial dysfunction results in an abnormal function and the apoptosis of pancreatic beta cells [23]. The intracellular ATP levels in the palmitate-treated cells with or without ADLE were measured to determine if the mitochondrial function is related to the anti-apoptotic effects of ADLE. As shown in Fig. 6B, incubating the INS-1 cells with palmitate for 24 h decreased the intracellular ATP levels by 60% compared to the control cells ( $P < 0.001$ ). On the other hand, a combination of palmitate and ADLE treatment increased the ATP levels by 20% compared to the palmitate only treated cells ( $P < 0.05$ ).

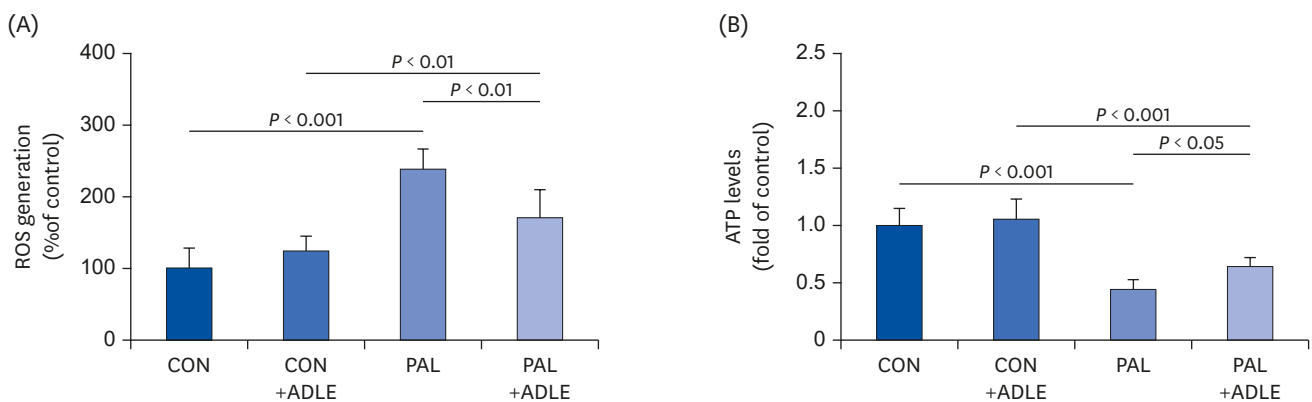


**Fig. 6.** ADLE treatment partially prevents ROS generation and restores the ATP levels reduced by palmitate in INS-1 cells. INS-1 cells were treated with 0.4 mM PAL in the absence or presence of 0.5 mg/mL ADLE. The cells were harvested, and (A) ROS and (B) intracellular ATP levels were examined. Data represent the mean  $\pm$  SD ( $n = 3-5$ ). Significance was evaluated using an ANOVA with the LSD comparisons test. ADLE, *Allomyrina dichotoma* larva extract; CON, untreated control; PAL, 0.4 mM palmitate only; CON+ADLE, untreated control plus 0.5 mg/mL ADLE; PAL+ADLE, 0.4 mM palmitate plus 0.5 mg/mL ADLE; ROS, reactive oxygen species; ATP, adenosine triphosphate; ANOVA, analysis of variance; LSD, Least Significant Difference.

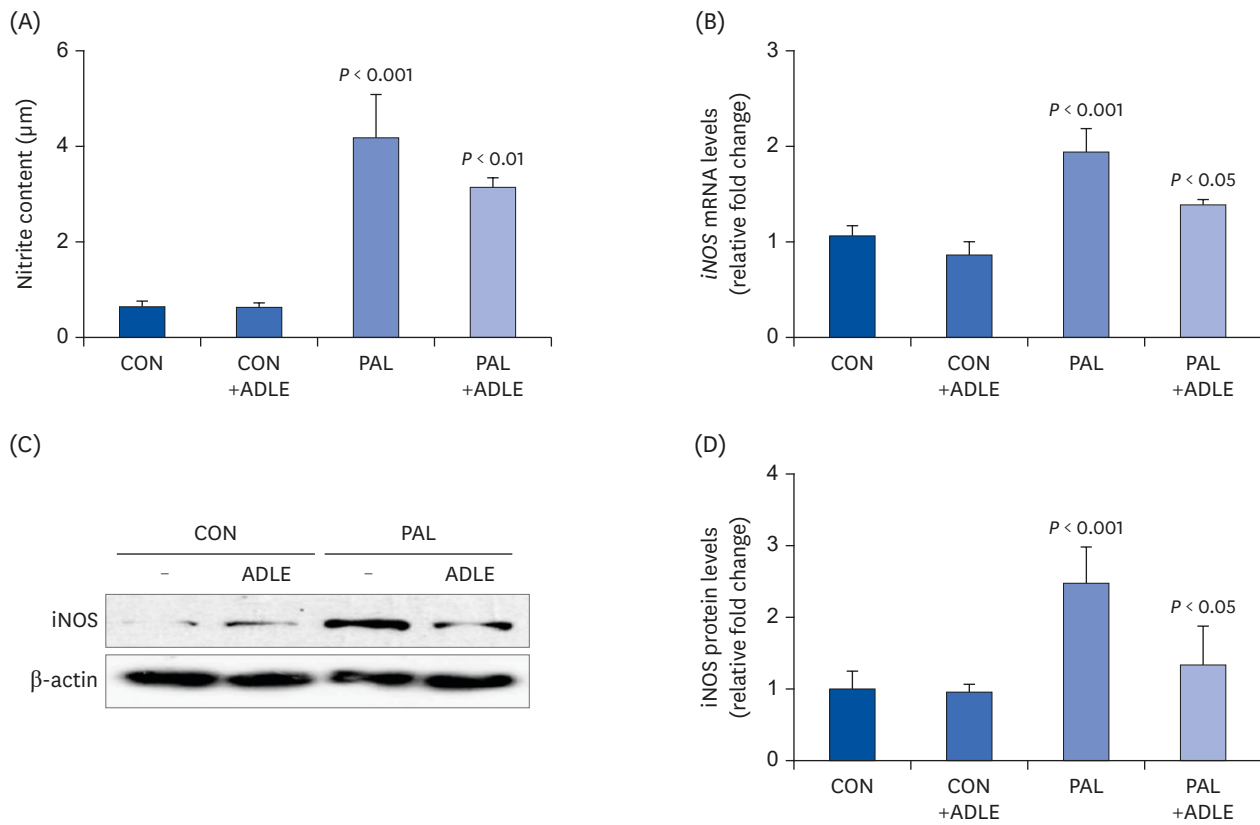


**Fig. 7.** ADLE treatment reduces palmitate-induced iNOS expression and nitrite in INS-1 cells. INS-1 cells were treated with 0.4 mM PAL in the absence or presence of 0.5 mg/mL ADLE. The cells were harvested after 16 h of treatment. (A) The nitrite content was measured in the cell-free culture supernatants. (B) The mRNA levels of *iNOS* were analyzed by quantitative RT-PCR. The mRNA levels were normalized to those of cyclophilin. (C, D) The iNOS protein level was determined by western blotting. The Western blotting data are representative of three independent experiments. The bands were quantified using Quantity 1 software. The significance was evaluated using an ANOVA with the LSD comparisons test. The data represent mean  $\pm$  SD ( $n = 3-5$ ). ADLE, *Allomyrina dichotoma* larva extract; CON, untreated control; PAL, 0.4 mM palmitate only; CON+ADLE, untreated control plus 0.5 mg/mL ADLE; PAL+ADLE, 0.4 mM palmitate plus 0.5 mg/mL ADLE; iNOS, inducible nitric oxide synthase; ANOVA, analysis of variance; LSD, Least Significant Difference.

### ADLE treatment reduces palmitate-induced iNOS expression and nitrite in INS-1 cells

The inflammatory response of beta cells stimulates the expression of inducible nitric oxide synthase and the overproduction of NO, resulting in cell damage [24]. Therefore, the nitrite concentration and the *iNOS* mRNA and protein levels in the supernatant of the culture medium and cell lysates were measured. As shown in **Fig. 7A**, incubation of INS-1 cells with palmitate for 24 h resulted in a 21-fold ( $P < 0.001$ ) increase in nitrite compared to the control cells. Similarly, ADLE reduced the nitrite concentration significantly ( $P < 0.01$ ). A significant increase ( $P < 0.001$ ) in the mRNA and protein expression levels of iNOS in INS-1 cells incubated with palmitate was observed, but this increase was suppressed significantly ( $P < 0.01$ ) by the ADLE treatment (**Fig. 7B and C**). The quantitative data also showed that iNOS/ $\beta$ -actin was significantly higher in palmitate-treated cells than the control cells, but these were inhibited by the ADLE treatment (**Fig. 7D**).

## DISCUSSION

Inadequate insulin secretion causes insulin resistance, which is a key issue in the development of diabetes [25]. Numerous studies have reported that acute FFA exposure

increases insulin release in pancreatic beta cells. On the other hand, prolonged FFA exposure causes disturbances in lipid metabolism regulation, contributing to decreased beta-cell function and viability (lipotoxicity) [26-28]. A previous study reported that ADLE ameliorates hepatic insulin resistance by inhibiting hepatic lipogenesis through the AMPK signaling pathway in HFD-induced mice [10]. In that study, glucose tolerance was also improved in the ADLE-treated mice, suggesting that ADLE has a positive effect on pancreatic beta cells. Therefore, this study examined the direct effect of ADLE on pancreatic islets compensation, insulin secretion, and beta-cell apoptosis in HFD-treated mice and palmitate-treated INS-1 cells. Under insulin-resistant conditions, an increase in beta-cell mass compensates for the increased demand in the maintenance of normal glucose homeostasis [29]. In the present study, the results obtained both *in vivo* and *in vitro* show that the beta-cell function and number of cells increase markedly in response to the ADLE treatment, which correlates with the results of metformin used as a type 2 diabetes therapy [30]. The prolonged exposure of isolated islets or insulin-secreting cells to elevated FAA levels is associated with the inhibition of GSIS and the induction of cell death by apoptosis [5].

Pepin *et al.* [31] reported that the p-AMPK/AMPK ratio decreased in the islets of diabetic mice compared to normal mice, both under low and high glucose conditions. In the present study, the AMPK activation was decreased in palmitate-treated cells, while AMPK phosphorylation was induced by a pretreatment with ADLE. These results suggest that the activation of AMPK by ADLE is one mechanism used to protect pancreatic islet cells from lipotoxicity and improve insulin secretion. Compared to the untreated cells, cells cultured for seven days in the presence of high levels of FFA exhibit the hallmarks of apoptosis, including DNA fragmentation, increased caspase activity, and increased expression of apoptotic genes [24]. In this study, the expression of apoptotic markers in palmitate-treated cells was increased. Furthermore, the ADLE treatment attenuated cleaved PARP, cleaved caspase-3, and the Bax/Bcl2 ratio. These results are consistent with those observed in the islets of HFD-induced diabetic mice treated with ADLE, which exhibited reduced oxidative stress and apoptotic cell death. Therefore, the insulin secretion capacity, and the anti-apoptotic effect, might be mechanisms through which ADLE induces a significant decrease in glucose tolerance, as observed in the HFD-treated mice.

The mitochondria play an essential role in ATP synthesis, Ca<sup>2+</sup> homeostasis, and the integration of apoptotic signals [32]. In beta cells, glucose sensing and subsequent insulin secretion were controlled by the mitochondrial metabolism [33]. ADLE improved GSIS and inhibited the oxidative stress-mediated pathway, as shown by the decrease in ROS generation and the increase in ATP content in the mitochondria. Therefore, the ADLE-induced mitochondrial functional recovery contributes to the anti-apoptotic effects and the recovery of the insulin secretory capacity of ADLE against lipotoxicity.

NO is a mediator of FFA-induced beta-cell dysfunction [34]. Therefore, this study investigated whether ADLE regulates NO. As expected, FFA (palmitate) induced NO production, which was ameliorated after a treatment with ADLE. Excessive NO production derived from iNOS has been associated with beta-cell dysfunctions by inflammation [35, 36, 37]. Previously, ADLE had anti-inflammatory activity in lipopolysaccharide (LPS)-induced Caco-2 cells by decreasing NO production and inflammatory cytokines [38]. In this study, ADLE reduced ROS production in palmitate-treated INS-1 cells, inhibiting the production of NO via a reduction in the iNOS protein levels. These findings suggest that ADLE plays an important role in beta-cell lipotoxicity through ROS/NO production.

Thirteen fractionations were obtained to elucidate the bioactive compounds of ADLE. A specific fraction exhibited low 2,2-diphenyl-1-picrylhydrazyl (DPPH) scavenging activity (data not shown), where DPPH acts as a free radical scavenger and has antioxidant activity. An attempt was made to isolate the compound with high antioxidant effects. Im *et al.* [14] also reported that ADLE increases the level of antioxidant enzymes, such as superoxide dismutase (SOD) and catalase (CAT), to provide protection against ROS generation induced by ultraviolet B (UVB) exposure in hairless mice. Therefore, a decrease in the levels of oxidative stress could be a key mechanism in ameliorating the anti-apoptotic effect, but more detailed studies will be needed to characterize the mechanisms of ADLE. Moreover, determining the circulating levels of several ADLE components in the mice will help elucidate how ADLE interacts with the body while also providing insights into its applicability for the development of food or drugs to treat glucose intolerance. On the other hand, studies must first be conducted to characterize the anti-apoptotic effects in human subjects, as well as determine the optimal doses and their tolerability in humans.

In conclusion, ADLE inhibits lipoapoptosis in beta cells by reducing the levels of NO and oxidative stress. Therefore, it can be used to help maintain beta-cell survival and preserve the capacity of insulin secretion.

## REFERENCES

1. Leonardi O, Mints G, Hussain MA. Beta-cell apoptosis in the pathogenesis of human type 2 diabetes mellitus. *Eur J Endocrinol* 2003;149:99-102.  
[PUBMED](#) | [CROSSREF](#)
2. Danial NN, Korsmeyer SJ. Cell death: critical control points. *Cell* 2004;116:205-19.  
[PUBMED](#) | [CROSSREF](#)
3. Strasser A. The role of BH3-only proteins in the immune system. *Nat Rev Immunol* 2005;5:189-200.  
[PUBMED](#) | [CROSSREF](#)
4. Wong WW, Puthalakath H. Bcl-2 family proteins: the sentinels of the mitochondrial apoptosis pathway. *IUBMB Life* 2008;60:390-7.  
[PUBMED](#) | [CROSSREF](#)
5. Oh YS, Bae GD, Baek DJ, Park EY, Jun HS. Fatty acid-induced lipotoxicity in pancreatic beta-cells during development of type 2 diabetes. *Front Endocrinol (Lausanne)* 2018;9:384.  
[PUBMED](#) | [CROSSREF](#)
6. Pemberton RW. Insects and other arthropods used as drugs in Korean traditional medicine. *J Ethnopharmacol* 1999;65:207-16.  
[PUBMED](#) | [CROSSREF](#)
7. Meyer-Rochow VB. Ethno-entomological observations from North Korea (officially known as the "Democratic People's Republic of Korea"). *J Ethnobiol Ethnomed* 2013;9:7.  
[PUBMED](#) | [CROSSREF](#)
8. Kim DS, Huh J, You GC, Chae SC, Lee OS, Lee HB, Lee JB, Kim JS. *Allomyrina Dichotoma* Larva extracts protect streptozotocin-induced oxidative cytotoxicity. *J Environ Toxicol* 2007;22:349-55.
9. Sagisaka A, Miyano-shita A, Ishibashi J, Yamakawa M. Purification, characterization and gene expression of a glycine and proline-rich antibacterial protein family from larvae of a beetle, *Allomyrina dichotoma*. *Insect Mol Biol* 2001;10:293-302.  
[PUBMED](#) | [CROSSREF](#)
10. Kim K, Bae GD, Lee M, Park EY, Baek DJ, Kim CY, Jun HS, Oh YS. *Allomyrina dichotoma* Larva extract ameliorates the hepatic insulin resistance of high-fat diet-induced diabetic mice. *Nutrients* 2019;11:1522.  
[PUBMED](#) | [CROSSREF](#)
11. Bégin-Heick N. Of mice and women: the beta 3-adrenergic receptor leptin and obesity. *Biochem Cell Biol* 1996;74:615-22.  
[PUBMED](#) | [CROSSREF](#)

12. Mauvais-Jarvis F. Role of sex steroids in  $\beta$  cell function, growth, and survival. *Trends Endocrinol Metab* 2016;27:844-55.  
[PUBMED](#) | [CROSSREF](#)
13. Díaz A, López-Grueso R, Gambini J, Monleón D, Mas-Bargues C, Abdelaziz KM, Viña J, Borrás C. Sex differences in age-associated type 2 diabetes in rats-role of estrogens and oxidative stress. *Oxid Med Cell Longev* 2019;2019:6734836.  
[PUBMED](#) | [CROSSREF](#)
14. Im AR, Ji KY, Park I, Lee JY, Kim KM, Na M, Chae S. Anti-photoaging effects of four insect extracts by downregulating matrix metalloproteinase expression via mitogen-activated protein kinase-dependent signaling. *Nutrients* 2019;11:1159.  
[PUBMED](#) | [CROSSREF](#)
15. Yoon YI, Chung MY, Hwang JS, Han MS, Goo TW, Yun EY. *Allomyrina dichotoma* (Arthropoda: Insecta) larvae confer resistance to obesity in mice fed a high-fat diet. *Nutrients* 2015;7:1978-91.  
[PUBMED](#) | [CROSSREF](#)
16. Gotoh M, Maki T, Satomi S, Porter J, Bonner-Weir S, O'Hara CJ, Monaco AP. Reproducible high yield of rat islets by stationary in vitro digestion following pancreatic ductal or portal venous collagenase injection. *Transplantation* 1987;43:725-30.  
[PUBMED](#) | [CROSSREF](#)
17. Folch J, Lees M, Sloane Stanley GH. A simple method for the isolation and purification of total lipides from animal tissues. *J Biol Chem* 1957;226:497-509.  
[PUBMED](#) | [CROSSREF](#)
18. Frijhoff J, Winyard PG, Zarkovic N, Davies SS, Stocker R, Cheng D, Knight AR, Taylor EL, Oettrich J, Ruskovska T, Gasparovic AC, Cuadrado A, Weber D, Poulsen HE, Grune T, Schmidt HH, Ghezzi P. Clinical relevance of biomarkers of oxidative stress. *Antioxid Redox Signal* 2015;23:1144-70.  
[PUBMED](#) | [CROSSREF](#)
19. Tamura K, Minami K, Kudo M, Iemoto K, Takahashi H, Seino S. Liraglutide improves pancreatic beta cell mass and function in alloxan-induced diabetic mice. *PLoS One* 2015;10:e0126003.  
[PUBMED](#) | [CROSSREF](#)
20. Kwon G, Pappan KL, Marshall CA, Schaffer JE, McDaniel ML. cAMP Dose-dependently prevents palmitate-induced apoptosis by both protein kinase A- and cAMP-guanine nucleotide exchange factor-dependent pathways in  $\beta$ -cells. *J Biol Chem* 2004;279:8938-45.  
[PUBMED](#) | [CROSSREF](#)
21. Kim JE, Song SE, Kim YW, Kim JY, Park SC, Park YK, Baek SH, Lee IK, Park SY. Adiponectin inhibits palmitate-induced apoptosis through suppression of reactive oxygen species in endothelial cells: involvement of cAMP/protein kinase A and AMP-activated protein kinase. *J Endocrinol* 2010;207:35-44.  
[PUBMED](#) | [CROSSREF](#)
22. Nakamura S, Takamura T, Matsuzawa-Nagata N, Takayama H, Misu H, Noda H, Nabemoto S, Kurita S, Ota T, Ando H, Miyamoto K, Kaneko S. Palmitate induces insulin resistance in H4IIEC3 hepatocytes through reactive oxygen species produced by mitochondria. *J Biol Chem* 2009;284:14809-18.  
[PUBMED](#) | [CROSSREF](#)
23. Lowell BB, Shulman GI. Mitochondrial dysfunction and type 2 diabetes. *Science* 2005;307:384-7.  
[PUBMED](#) | [CROSSREF](#)
24. Shimabukuro M, Zhou YT, Levi M, Unger RH. Fatty acid-induced beta cell apoptosis: a link between obesity and diabetes. *Proc Natl Acad Sci U S A* 1998;95:2498-502.  
[PUBMED](#) | [CROSSREF](#)
25. Schofield CJ, Sutherland C. Disordered insulin secretion in the development of insulin resistance and type 2 diabetes. *Diabet Med* 2012;29:972-9.  
[PUBMED](#) | [CROSSREF](#)
26. Ayvaz G, Balos Törüner F, Karakoç A, Yetkin I, Cakir N, Arslan M. Acute and chronic effects of different concentrations of free fatty acids on the insulin secreting function of islets. *Diabetes Metab* 2002;28:3S7-12.  
[PUBMED](#)
27. Fujiwara K, Maekawa F, Yada T. Oleic acid interacts with GPR40 to induce  $Ca^{2+}$  signaling in rat islet  $\beta$ -cells: mediation by PLC and L-type  $Ca^{2+}$  channel and link to insulin release. *Am J Physiol Endocrinol Metab* 2005;289:E670-7.  
[PUBMED](#) | [CROSSREF](#)
28. Barlow J, Jensen VH, Jastroch M, Affourtit C. Palmitate-induced impairment of glucose-stimulated insulin secretion precedes mitochondrial dysfunction in mouse pancreatic islets. *Biochem J* 2016;473:487-96.  
[PUBMED](#) | [CROSSREF](#)

29. Weir GC, Laybutt DR, Kaneto H, Bonner-Weir S, Sharma A. Beta-cell adaptation and decompensation during the progression of diabetes. *Diabetes* 2001;50 Suppl 1:S154-9.  
[PUBMED](#) | [CROSSREF](#)
30. Tajima K, Shirakawa J, Okuyama T, Kyohara M, Yamazaki S, Togashi Y, Terauchi Y. Effects of metformin on compensatory pancreatic  $\beta$ -cell hyperplasia in mice fed a high-fat diet. *Am J Physiol Endocrinol Metab* 2017;313:E367-80.  
[PUBMED](#) | [CROSSREF](#)
31. Pepin É, Al-Mass A, Attané C, Zhang K, Lamontagne J, Lussier R, Madiraju SR, Joly E, Ruderman NB, Sladek R, Prentki M, Peyot ML. Pancreatic  $\beta$ -cell dysfunction in diet-induced obese mice: roles of AMP-kinase, protein kinase C $\epsilon$ , mitochondrial and cholesterol metabolism, and alterations in gene expression. *PLoS One* 2016;11:e0153017.  
[PUBMED](#) | [CROSSREF](#)
32. Wiederkehr A, Wollheim CB. Minireview: implication of mitochondria in insulin secretion and action. *Endocrinology* 2006;147:2643-9.  
[PUBMED](#) | [CROSSREF](#)
33. Maechler P, Li N, Casimir M, Vetterli L, Frigerio F, Brun T. Role of mitochondria in beta-cell function and dysfunction. *Adv Exp Med Biol* 2010;654:193-216.  
[PUBMED](#) | [CROSSREF](#)
34. Shimabukuro M, Ohneda M, Lee Y, Unger RH. Role of nitric oxide in obesity-induced beta cell disease. *J Clin Invest* 1997;100:290-5.  
[PUBMED](#) | [CROSSREF](#)
35. Salehi A, Carlberg M, Henningson R, Lundquist I. Islet constitutive nitric oxide synthase: biochemical determination and regulatory function. *Am J Physiol* 1996;270:C1634-41.  
[PUBMED](#) | [CROSSREF](#)
36. Tsuura Y, Ishida H, Shinomura T, Nishimura M, Seino Y. Endogenous nitric oxide inhibits glucose-induced insulin secretion by suppression of phosphofructokinase activity in pancreatic islets. *Biochem Biophys Res Commun* 1998;252:34-8.  
[PUBMED](#) | [CROSSREF](#)
37. Akesson B, Henningson R, Salehi A, Lundquist I. Islet constitutive nitric oxide synthase and glucose regulation of insulin release in mice. *J Endocrinol* 1999;163:39-48.  
[PUBMED](#) | [CROSSREF](#)
38. Kim K, Bae GD, Park EY, Baek DJ, Kim CY, Jang SE, Oh YS. *Allomyrina dichotoma* larval extract attenuates intestinal barrier disruption by altering inflammatory response and tight junction proteins in lipopolysaccharide-induced Caco-2 cells. *Biochem Biophys Res Commun* 2020;532:145-50.  
[PUBMED](#) | [CROSSREF](#)